Journal of Electroceramics, 15, 75–81, 2005


# Electrical Behavior of $BaO$-$Nd_2O_3$-$Sm_2O_3$-$TiO_2$ with Glass/Oxide Additives Analyzed by Impedance Spectroscopy

LI-CHUN CHANG[1] & BI-SHIOU CHIOU[1,2,*]

[1]*Department of Electronics Engineering and Institute of Electronics,*
[2]*Innovation Packaging Research Center, National Chiao Tung University, 1001 Ta Hsueh Rd., Hsinchu, 300, Taiwan, R.O.C.*

Submitted February 12, 2003; Revised November 15, 2004; Accepted March 23, 2005

**Abstract.** The electrical properties of $BaO$-$Nd_2O_3$-$Sm_2O_3$-$TiO_2$ ceramics doped with low loss glass or low melting point oxide $B_2O_3$ are evaluated by impedance spectroscopy. Glass or $B_2O_3$ is doped as liquid phase sintering aid. Doping of glass/$B_2O_3$ enhances both the growth in the longitudinal direction of the columnar crystal and the preferred orientation of (002). The grain size increases and grain boundary decreases with the increase of dopant. Both the grain and grain-boundary resistivities decrease with the increase of dopant. The grain boundary activation energy for charge transport is larger than that of the grain activation energy. Possible mechanisms for the electrical behavior of the liquid-phase sintered $BaO$-$Nd_2O_3$-$Sm_2O_3$-$TiO_2$ ceramics are proposed and discussed.

**Keywords:** impedance spectroscopy, microwave, dielectric, electrical properties, liquid phase sintering, sintering aid

## 1. Introduction

$BaO$-($Ln_2O_3$, Ln = La, Nd, and Sm)-$TiO_2$ system has excellent dielectric properties for dielectric resonator applications used in the microwave telecommunication such as mobile telephone systems and satellite broadcasting [1]. These properties are high quality factor ($Q \times f$) near 9000 GHz, high dielectric constant ($\varepsilon_r$) about 80, and low temperature coefficient of resonant frequency ($\tau_f$) around +9 ppm/°C for $BaO$-($Nd_2O_3$, $Sm_2O_3$)-$TiO_2$ (hereafter referred to as BNST) system [2]. However, BNST ceramics have to be sintered at 1400°C, and therefore only platinum or refractory metals can be used as the inner conductors. These metals are expensive, their electrical performances are poor, and the cost-effective fabrication of high-quality components is thus difficult. Reduction of the sintering temperature of BNST to 960°C would enable the use of less expensive and better electrode materials, such as, silver. Furthermore, low temperature sintering would allow true integration of such BNST components with low temperature co-fired ceramic (LTCC) structures in a most convenient way.

A common method to decrease the sintering temperature of ceramic materials is to add some glass or low melting point materials [3, 4]. The liquid that formed during sintering promotes densification and grain coarsening at lower temperatures, but these additives generally degrade electrical properties if not selected properly. With an appropriate addition of $B_2O_3$, the sintering temperature of the BNST ceramic is reduced by 200°C [4–6]. The dielectric properties of the $B_2O_3$-doped dielectrics sintered at lower temperature were commensurate with that of un-doped ones sintered at higher temperature.

This is a continuing research, in our previous work [7, 8], the effects of glass (a low loss $Al_2O_3$-doped silica glass abbreviated as AS-glass) and $B_2O_3$ addition on the sintering behavior and dielectric microwave properties of BNST have been investigated. It is found that $B_2O_3$ addition reduces the sintering temperature to below 1020°C. Besides, specimens with sintering aids exhibit columnar structure and significant (002) preferred orientation. However, the correlation between the columnar structure and the dielectric property of

*To whom all correspondence should be addressed. E-mail: lcchang.ee87g@nctu.edu.tw; bschiou@mail.nctu.edu.tw

the ceramic is not clear. In this work, the effects of the columnar grain on the electrical properties are investigated with impedance spectroscopy.

## 2. Experimental Procedures

A BNST-based powder supplied by Phycomp Inc. was used as the starting material. An $Al_2O_3$-doped silica glass designed as AS-glass and $B_2O_3$(>99%) powders are employed as additives in this study. Host materials were mixed with either AS-glass or boric oxide in distilled water. In the case of $B_2O_3$doped system, the mixture was stirred at 90°C for 3 hr and then cooled to room temperature. The mixture was milled for 12 hr with zirconia balls. After milling, the slurry was dehydrated and granulated by mixing with 3 wt% polyvinyl alcohol solution. Pellets with 10 mm in diameter and 5.5 mm or 1.2 mm in thickness were pressed using uniaxial pressing. A pressure of 750 kg/cm$^2$ was used for all samples. After debinding, sintering was carried out in air at a temperature range of 1000 to 1250°C in the case of AS-glass doped BNST, 900 to 1100°C in the case of $B_2O_3$ doped BNST, and 1000 to 1450°C in the case of undoped BNST ceramics.

The X-ray diffraction spectra were collected by using Cu $K_\alpha$ ($\lambda = 0.15406$ nm) radiation with 30 kV and 20 mA in the $2\theta$ range of 20° to 50° (XRD, MAC Science MXP18), the intensity of the main peak was then integrated. The microstructure observations of sintered samples were performed with a scanning electron microscope (SEM, Hitachi S4700). An electron probe microanalyzer (EPMA, Joel JXA-8800M) was used to analyze the composition of the sintered samples. The bulk densities of the sintered specimens were measured by the Archimedes' method. According to the rule of mixing, the density of BNST ceramics is:

$$D_{\text{cal}} = (W_1 + W_2)/(W_1/D_1 + W_2/D_2) \qquad (1)$$

where $W_1$ and $W_2$ are the weight per cent of the BNST dielectric and AS-glass/$B_2O_3$ in the mixtures, respectively; $D_1$ and $D_2$ are the densities of the BNST and AS-glass/$B_2O_3$, respectively.

Silver electrodes were initially painted on both faces of the samples and cured at 600°C for 15 min to ensure good electrical contacts. Impedance analysis was performed using an Impedance/Gain-Phase Analyzer (Hewlett Packard HP4194), controlled by a PC, which covers a frequency range between 100 Hz and 15 MHz. Measurements were made at the temperature range of 25 to 350°C. The Cole-Cole diagrams are then plotted. The complex impedance $Z$ of the specimen is expressed as $Z' = Z + jZ''$. An equivalent circuit model was proposed on the basis of the $Z''$ versus $Z'$ plot. The dielectric constant and resistivity of the specimen were calculated from the measured capacitance and resistance, respectively.

## 3. Results and Discussions

Figure 1 shows the XRD patterns of some BNST specimens with and without additives. The (511) peak is the main characteristic peak of the phase of undoped ceramics. While for both AS-glass and boric oxide doped BNST, the (002) peak is more prominent than the (511) peak, as exhibited in Fig. 1(b) and (c), respectively. Table 1 summarizes the sample designation, additive concentration, sintering conditions, lattice parameters, unit cell volume, and relative unit cell volume of the specimens in this study. Specimens are designated as $A - T$, where $A$ represents the additive type and concentration and $T$ is the sintering temperature in °C. As shown in Table 1, the lattice parameters a

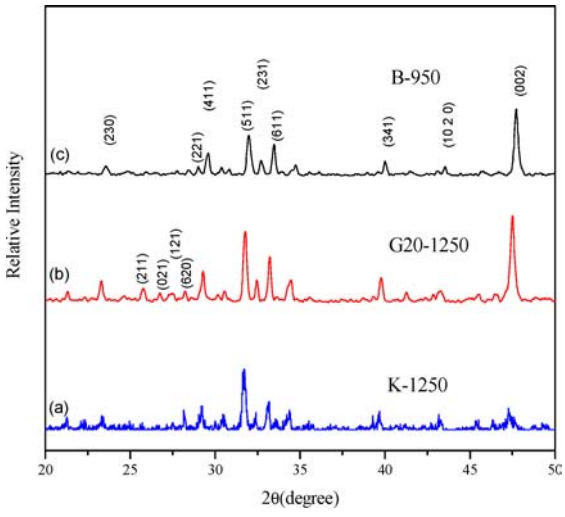


*Fig. 1.* XRD patterns for BNST ceramics (a) without additive, sintered at 1250°C for 2 hr, (b) with 20 wt% AS-glass, sintered at 1250°C for 2 hr, and (c) with 2 wt% $B_2O_3$ sintered at 950°C for 1 hr.

*Table 1.* The sample designation, additive concentration, sintering conditions, lattice parameters, unit cell volume, and relative unit cell volume of BNST specimens in this study.

| Sample designation $A$-$T$* | Additive concentration | Lattice parameters: Sintering conditions | $a$ (Å) | $b$ (Å) | $c$ (Å) | Unit cell volume (Å$^3$) | Relative unit cell volume $V/V_{k\text{-}1050}$ |
|---|---|---|---|---|---|---|---|
| K-1050 | 0 | 1050°C, 1 hr | 21.469 | 12.007 | 3.922 | 1011.1 | 1.000 |
| K-1250 | 0 | 1250°C, 1 hr | 21.894 | 12.008 | 3.874 | 1018.5 | 1.007 |
| G5-1050 | 5 wt% AS glass | 1050°C, 1 hr | 21.805 | 12.003 | 3.882 | 1016.1 | 1.005 |
| G10-1050 | 10 wt% AS glass | 1050°C, 1 hr | 22.044 | 12.088 | 3.838 | 1022.7 | 1.011 |
| G5-1250 | 5 wt% AS glass | 1250°C, 1 hr | 21.985 | 12.101 | 3.863 | 1027.7 | 1.016 |
| G10-1250 | 10 wt% AS glass | 1250°C, 1 hr | 22.117 | 12.118 | 3.829 | 1026.2 | 1.015 |
| B1-1050 | 1 wt% $B_2O_3$ | 1050°C, 1 hr | 22.368 | 12.262 | 3.775 | 1035.3 | 1.024 |
| B2-1050 | 2 wt% $B_2O_3$ | 1050°C, 1 hr | 22.531 | 12.218 | 3.745 | 1030.8 | 1.019 |
| B5-1050 | 5 wt% $B_2O_3$ | 1050°C, 1 hr | 22.452 | 12.293 | 3.761 | 1035.2 | 1.024 |

*$A$:additive type and concentration, $T$: sintering temperature in °C.

and b increase while c slightly decreases with boric oxide/AS-glass content. A small increase of the unit cell volume is observed for the doped specimens. The $B_2O_3$-doped ceramics exhibit larger volume increase than the AS-added BNST's do. Our previous work [8] suggests that: there was no specific boron compound observed at grain boundaries in sintered specimens, and the EPMA (crystal number: LDE2H0094/JEOL LTD., average $2d = 9.77$ nm, gives a resolution of 0.001%) analysis results indicated that the boron content of the sintered specimens was same as that of the unsintered-sample. Besides, the unit cell volumes of $B_2O_3$-doped specimens are larger than those of the undoped ones, as listed in Table 1. The atomic radii of B, Ba, Nd, Sm, Ti and O are 0.023, 0.136, 0.100, 0.096, 0.061, and 0.14 nm, respectively. If the small boron atoms would incorporate into the lattice sites, a decrease, instead of increase, of the unit cell volume will be observed. Hence, it is argued that the increase of the unit cell volume for specimens sintered at higher temperature and/or doped with more $B_2O_3$ is attributed to the diffusion of B atoms to the interstitial sites. In addition, our previous work revealed the existence of glassy phase between BNST grains when too much glass is added [7]. The surface SEM micrographs indicate that samples sintered at higher temperatures and/or with additives exhibit columnar grains with a high ratio of length ($l$) to diameter ($\phi$) as shown in Fig. 2 and summarized in Table 2. The columnar structure is more obvious for samples sintered at high temperatures. The $l/\phi$'s are 11.22, 9.44, and 17.17 for the undoped-BNST sintered at 1450°C (K-1450), 5 wt% AS-BNST sintered at 1250°C (G5-1250), and 10 wt% AS-BNST sintered at 1250°C (G10-1250), respectively. Possibly because sintering at elevated temperatures is needed for grains to grow with preferred orientation via rearrangement.

*Table 2.* Peak ratio $I_{(002)\text{-}s}/I^*_{(002)\text{-}p}$, ratio of grain length to diameters ($l/\phi$), grain capacitance ($C_g$), grain boundary capacitance ($C_{gb}$), grain resistance ($R_g$), and grain boundary resistance ($R_{gb}$) of the samples.#,+

| Sample | Peak ratio ($I_{(002)-s}/I_{(002)-p}$) | $l/\phi$ (um/um) | $C_g$ ($10^{-11}$F) | $C_{gb}$ (10-$^9$F) | $R_g$ (Ω) | $R_{gb}$ ($10^4\Omega$) |
|---|---|---|---|---|---|---|
| K-1050 | 1.28 | 1.00 | 0.69 | 1.57 | 402 | 16.93 |
| K-1250 | 1.71 | 1.00 | 1.04 | 2.02 | 279 | 12.33 |
| K-1450 | 1.76 | 11.22 | 1.52 | 2.28 | 191 | 10.74 |
| G5-1050 | 1.82 | 1.05 | 1.10 | 2.53 | 175 | 5.23 |
| G10-1050 | 1.95 | 1.11 | 1.22 | 2.09 | 143 | 9.53 |
| G5-1250 | 2.82 | 9.44 | 1.64 | 3.21 | 105 | 4.06 |
| G10-1250 | 4.12 | 17.17 | 1.74 | 2.19 | 95 | 6.17 |
| Bl-1050 | 2.25 | 2.03 | 1.36 | 3.6 | 159 | 2.94 |
| B2-950 | 3.41 | 2.58 | 1.52 | 4.38 | 191 | 3.30 |
| B2-1000 | 5.16 | 4.28 | 1.82 | 4.76 | 163 | 2.98 |
| B2-1050 | 6.90 | 5.00 | 1.94 | 5.09 | 155 | 2.75 |

*$I_{(002)\text{-}s}/I_{(002)\text{-}p}$: the (002) peak intensity of the as-sintered specimen $I_{(002)\text{-}s}$ to that of the as-pressed specimen $I_{(002)\text{-}p}$.
# Sintering time is 1 hr in air.
+The capacitance and resistance from the impedance data measured at 350°C and analyzed with impedance spectroscopy.

Three typical impedance diagrams ($Z''$ versus $Z'$) of BNST ceramics are given in Fig. 3 which suggest loci of two semicircles for each sample. An equivalent

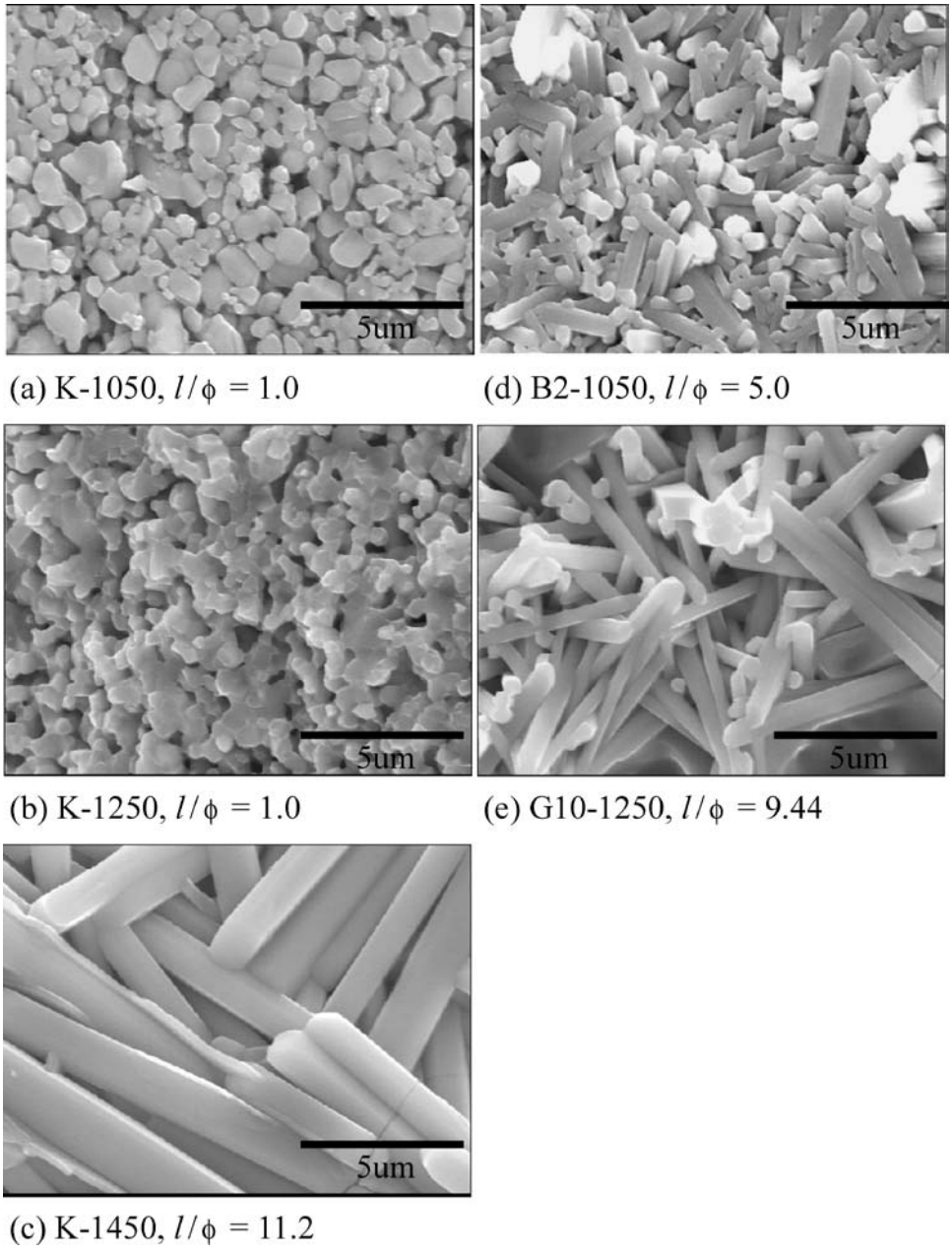


*Fig. 2.* Surface SEM micrographs and ratios of grain length to diameter ($l/\phi$) of undoped BNST ceramics sintered at (a) 1050°C, (b) 1250°C, (c) 1450°C, (d) BNST doped with 2 wt% $B_2O_3$ sintered at 1050°C, and (e) BNST doped with 10 wt% AS-glass sintered at 1250°C.

circuit model with two parallel *RC*'s in series is proposed. As indicated in Fig. 4, when $R_2C_2 \ll R_1C_1$, the impedance diagram of the equivalent circuit exhibits two distinct semicircles. The angular frequency $\omega_i$ is the frequency at the peak of the semicircle $i$ in the Cole-Cole diagram shown in Fig. 4(b). While the intercepts at $Z'$ axis give $R_1$ and $(R_1 + R_2)$ values, the capacitance $C_i$ is obtained using the equation $\omega_i = 1/R_iC_i$. The first semicircle, shown in Fig. 3(b), exhibits the high frequency ($>10^4$ Hz) impedance data and corresponds

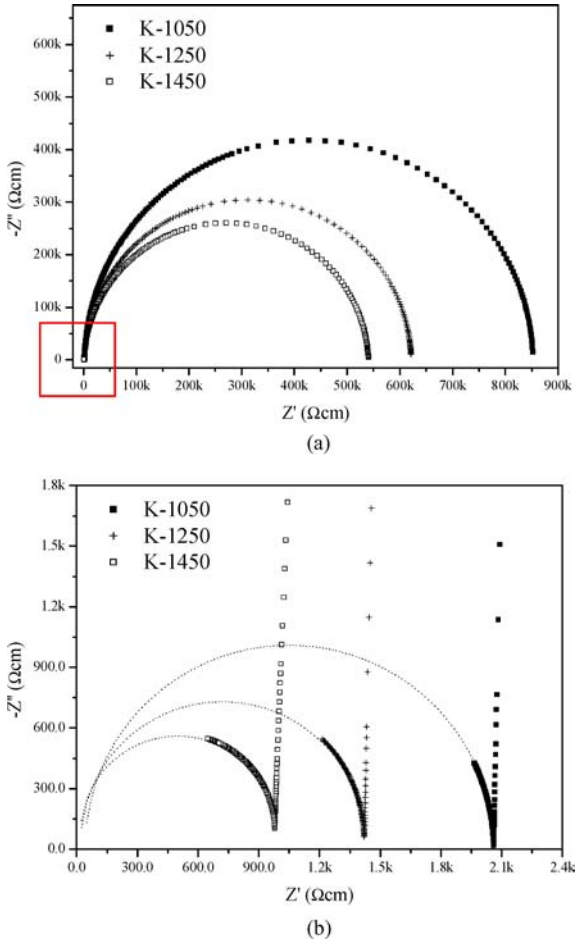


*Fig. 3.* (a) Typical impedance diagrams of undoped BNST sintered at various temperatures and (b) the enlargement of the plot inside the square area of (a). Impedance measured at 350°C.

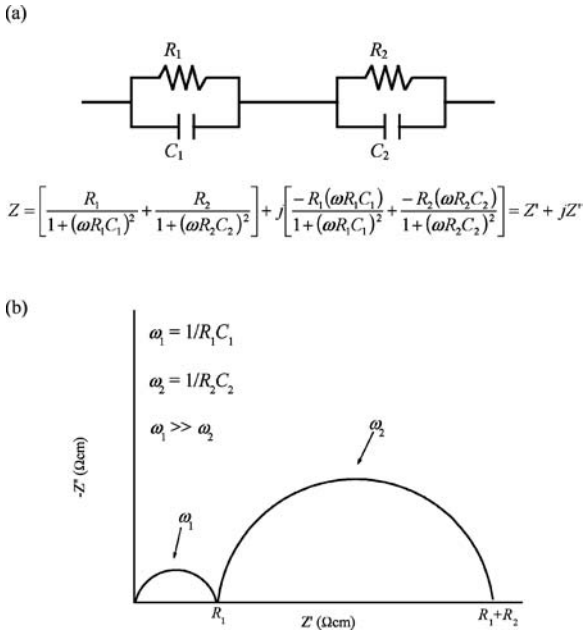


*Fig. 4.* Schematic diagram of two parallel $RC$'s in series, the complex impedance of the circuit is $Z$, and (b) the impedance diagram $-Z''$ vs $Z'$ of the circuit in (a), when $R_1C_1 \ll R_2C_2$.

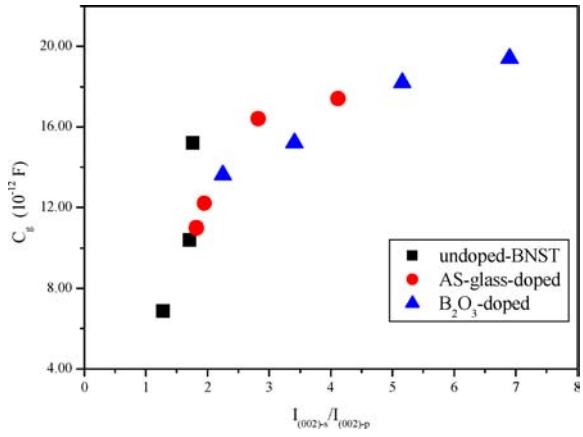


*Fig. 5.* Grain capacitance $C_g$ versus the (002) peak intensity ratio of the as-sintered sample to that of the as-pressed one, $I_{(002)\text{-}s}/I_{(002)\text{-}p}$.

to the dipole polarization of the lattice (bulk) material inside the grain, i.e., the resistance ($R_g$) and capacitance ($C_g$) attributed to the grains. The second semicircle, observed in the low frequency range ($10^2$–$10^4$ Hz) and/or at high measurement temperature (>300°C) represents space charge polarization at the grain boundaries ($R_{gb}$ and $C_{gb}$) [9]. Also summarized in Table 2 are the $R_g$, $C_g$, $R_{gb}$, and $C_{gb}$ obtained from the impedance plots of various specimens. In addition, the (002) peak intensity of the as-sintered specimen to the as-pressed one ($I_{(002)\text{-}s}/I_{(002)\text{-}p}$) is listed in Table 2. Figure 5 exhibit the $C_g$ versus peak ratio plot, the grain capacitance $C_g$ increases with the peak ratio $I_{(002)\text{-}s}/I_{(002)\text{-}p}$ for both the undoped BNST and doped BNST. The higher the (002) preferred orientation is, the larger the dielectric constant is. The peak ratios of samples K-1050, G10-1050, and B2-1050 are 1.28, 1.95, and 6.90, respectively. And the calculated grain dielectric constant

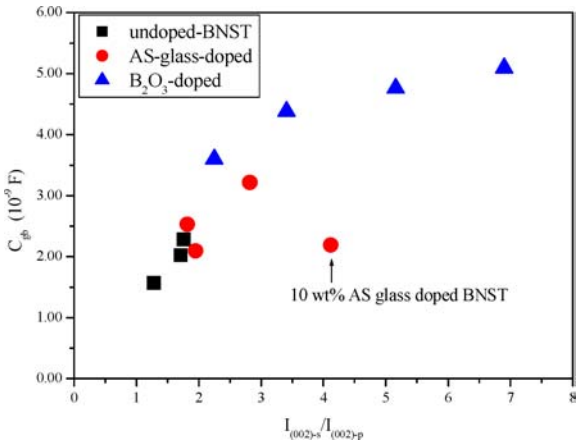


*Fig. 6.* Grain boundary capacitance $C_{gb}$ versus the (002) peak intensity ratio of the as-sintered sample to that of the as-pressed one, $I_{(002)\text{-}s}/I_{(002)\text{-}p}$. $C_{gb}$ increases with the increase of $I_{(002)\text{-}s}/I_{(002)\text{-}p}$, however, a drop in $C_{gb}$ is observed for specimens with too much glass (10 wt% AS glass) as indicated by arrow.

are 15.5(K-1050), 27.7(G10-1050) and 43.9(B2-1050). Similar trend is observed for the grain boundary capacitance $C_{gb}$ of the undoped and boric oxide doped specimens. The capacitance of the grain-boundary also increases with the ratio of $I_{(002)\text{-}s}/I_{(002)\text{-}p}$, as observed in Fig. 6. No clear correlation between the resistance (both $R_g$ and $R_{gb}$) and the peak ratio, i.e., the preferred (002) orientation, is observed.

Samples with AS glass contents of less than 5 wt% show an initial increase of $C_{gb}$ with the peak ratio, however, a drop in $C_{gb}$ is observed for the 10 wt% AS-doped ones. Our previous work revealed the existence of glassy phase between BNST grains when too much glass is added [7]. This is the root cause for the small $C_{gb}$ for specimens doped with 10 wt% AS-glass. The resistivity as a function of temperature is given in Fig. 7. Both the grain ($\rho_g$) and grain boundary ($\rho_{gb}$) resistivities decrease with the presence of the sintering aids. The presence of the sintering aid increases the dielectric loss. The grain boundary resistivity$\rho_{gb}$ of $B_2O_3$-doped sample is less than one-tenth of that of undoped ones. The grain resistivity decreases with the increase of additive content and/or the sintering temperature. As shown in Fig. 7, the 300°C $\rho_g$ of K-1050 ($7.83 \times 10^3$ Ωcm) is 2 times higher than that of G5-1050 ($3.58 \times 10^3$ Ωcm), and 4 times higher than that of G5-1250 ($1.97 \times 10^3$ Ωcm).

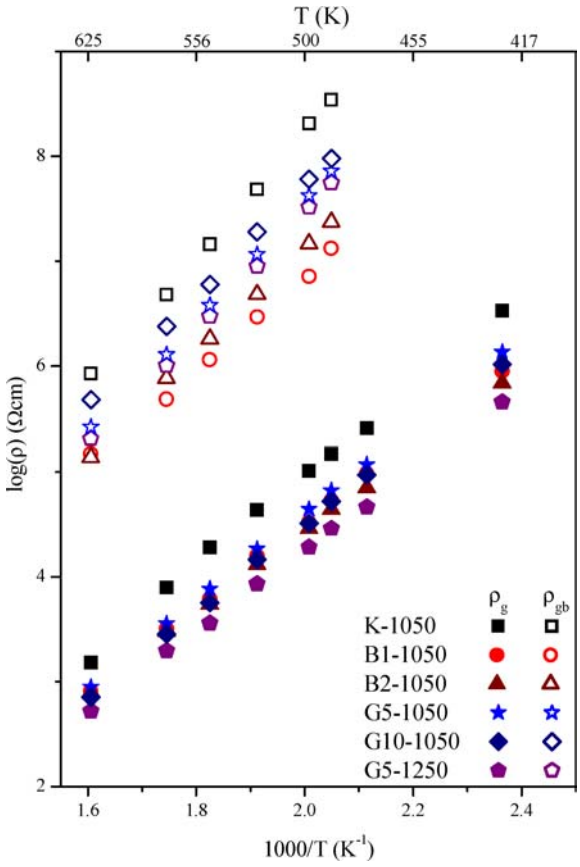


*Fig. 7.* Grain and grain boundary resistivities as a function of temperature.

The resistivity of the specimen is described by the Arrhenius equation:

$$\rho = \rho_0 \exp(\Delta E_a / kT) \tag{2}$$

where $\rho_0$ is the pre-exponential factor, $\Delta E_a$ is the activation energy for charge transportation and $k$ is the Boltzmann constant. The activation energy is obtained from the slope of the Arrhenius plot and summarized in Table 3. The grain boundary activation energy ($\Delta E_{a\text{-}gb}$) is larger than the grain activation energy ($\Delta E_{a\text{-}g}$) for all the specimens studied. There is a slight decrease of the activation energy for $B_2O_3$-doped samples. No apparent difference in the activation energy is observed between the undoped and glass-doped BNST ceramics. The grain activation energy ranges from 0.79 to 0.89 eV, and the grain boundary activation energy

*Table 3*. Activation energies for charge transport via the grain ($\Delta E_{a\text{-}g}$) and grain boundary ($\Delta E_{a\text{-}gb}$) of the BNST samples sintered in air for 1 hr.

| Sample | $\Delta E_{a\text{-}g}$ (eV) | $\Delta E_{a-gb}$ (eV) |
|---|---|---|
| K-1050 | $0.89 \pm 0.03$ | $1.18 \pm 0.03$ |
| K-1250 | $0.88 \pm 0.03$ | $1.08 \pm 0.03$ |
| K-1450 | $0.81 \pm 0.03$ | $1.05 \pm 0.03$ |
| G5-1050 | $0.86 \pm 0.03$ | $1.09 \pm 0.03$ |
| G10-1050 | $0.85 \pm 0.03$ | $1.12 \pm 0.03$ |
| G5-1250 | $0.81 \pm 0.03$ | $1.07 \pm 0.03$ |
| G10-1250 | $0.79 \pm 0.03$ | $1.11 \pm 0.03$ |
| Bl-1050 | $0.84 \pm 0.03$ | $0.90 \pm 0.03$ |
| B2-950 | $0.82 \pm 0.03$ | $0.95 \pm 0.03$ |
| B2-1000 | $0.83 \pm 0.03$ | $0.93 \pm 0.03$ |
| B2-1050 | $0.85 \pm 0.03$ | $0.91 \pm 0.03$ |

ranges from 0.90 to 1.18 eV. They are typical values of the activation energy for charge transportation in electronic ceramics [10].

## 4. Conclusions

In this study, glass or $B_2O_3$ is used to lower the sintering temperature of the BNST ceramics, and impedance spectroscopy is employed to analyze the electrical behavior of the specimens. Preferred (002) orientation and elongated grain structure are observed in samples doped with $B_2O_3$/glass and/or sintered at elevated temperatures. Both the grain capacitance $C_g$ and the dielectric constant increase with the increase of degree of preferred (002) orientation. Similar trend is observed for the grain boundary capacitance $C_{gb}$ of the undoped and $B_2O_3$-doped BNST ceramics. However, for glass-doped specimens, a decrease after the initial increase of $C_{gb}$ with the increase of preferred orientation is observed due to the presence of the glassy phase in the grain boundaries when too much glass is added. Both the grain ($\rho_g$) and grain boundary ($\rho_{gb}$) resistivities decrease with the presence of the sintering aids. The activation energies for charge transport via bulk material and via grain boundaries are derived from the Arrhenius plots of the $\rho_g$ versus $1/T$ and $\rho_{gb}$ versus $1/T$ curve, respectively. The grain boundary activation energy is larger than the grain activation energy for all the specimens studied.

## Acknowledgments

This work is sponsored by National Science Council, Taiwan, under the contract number NSC93-2216-E009-023.

## References

1. H. Ohsato, M. Imaeda, Y. Takagi, A. Komura, and T. Okuda, in *Proceedings of the Eleventh IEEE International Symposium on Applications of Ferroelectric*, (1998) p. 509.
2. P. Laffez, G. Desgardin, and B.Raveau, *J. Mater. Sci.*, **27**, 5229 (1992).
3. R.R. Tummala, *J. Am. Ceram. Soc.*, **74**, 895 (1991).
4. S.M. Rhim, S. Hong, H. Bak, and O.K. Kim, *J. Am. Ceram. Soc.*, **83**, 1145 (2000).
5. C.L. Huang and M.H. Weng, *Mater. Res. Bull.*, **36**, 2741 (2001).
6. P. Liu, E.S. Kim, S.G. Kang, and H.S. Jang, *Mater. Chem. Phy.*, **79**, 270 (2003).
7. L.C. Chang, B.S. Chiou, and W.H. Lee, *J. Mat. Sci.*: material in electronics, **15**, 153 (2004).
8. L.C. Chang and B.S. Chiou, *Journal of Electroceramics*, (in press).
9. B.S. Chiou, S.T. Lin, J.G. Duh, and P.H. Chang, *J. Am. Ceram. Soc.*, **72**, 1967 (1989).
10. Z.S. Macedo, C.R. Ferrari, and A.C. Hernandes, *J. Euro. Ceram. Soc.*, **24**, 2567 (2004).